

Rev. Fac. Ing. Univ. Antioquia N.º 49. pp. 61-69. Septiembre, 2009

Study of diesel sprays using computational fluid dynamics

Estudio de chorros diesel usando mecánica de fluidos computacional

John Agudelo^{1*}, Andrés Agudelo¹, Pedro Benjumea²

¹Group of Efficient Energy Management – GIMEL – Engineering Faculty, Universidad de Antioquia, Calle 67 N.º. 53-108, Medellín, Colombia.

²Alternative Fuels Group, Energy Institute, Faculty of Mines, Universidad Nacional de Colombia, Sede Medellín, Calle 59A N.º. 63-20, Colombia.

(Recibido el 25 de noviembre de 2008. Aceptado el 26 de mayo de 2009)

Abstract

In this work a numerical model for simulating the main sub-processes occurring in a fuel spray was developed using an open-source CFD code. The model was validated by comparing predicted dimethyl ether (DME) spray tip penetrations with experimental data reported in literature and some results obtained from empirical correlations. Once validated, the model was used for evaluating the effect of fuel type, injection pressure and ambient gas pressure on spray tip penetration, Sauter mean diameter (SMD) and evaporated fuel mass. Fuel properties significantly affected the atomization and evaporation processes and in a lesser extent spray fuel penetration. Regarding the injection and ambient gas pressures, the SMD increased with viscosity and surface tension while the evaporation rate increased with fuel volatility. At low ambient gas pressures the evaporation process was highly favored as well as the spray penetration. For both fuels, as injection pressure increased the SMD decreased and the evaporation rate increased.

----- *Keywords:* Fuel spray, atomization, vaporization, simulation.

Resumen

En este trabajo se desarrolló un modelo numérico para simular los principales subprocesos que ocurren en un chorro diesel usando un código CFD de libre acceso. El modelo se validó comparando valores predichos de la penetración de la punta del chorro para el dimetil éter (DME) con datos experimentales reportados en la literatura y resultados obtenidos a partir de correlaciones

* Autor de correspondencia: teléfono: + 57 + 4 + 219 8549, fax: + 57 + 4 211 0507, correo electrónico: jragude@udea.edu.co (J. Agudelo)

empíricas. Una vez validado, el modelo se usó para evaluar el efecto del tipo de combustible, la presión de inyección y la presión del gas ambiente en la penetración de la punta del chorro, el diámetro medio de Sauter (SMD) y la masa de combustible evaporada. Las propiedades del fluido afectaron significativamente los procesos de atomización y vaporización y en menor medida la penetración del chorro. Independientemente de las presiones de inyección y del gas ambiente, el SMD incrementó con la viscosidad y la tensión superficial mientras la tasa de evaporación incrementó con la volatilidad del combustible. A bajas presiones del gas ambiente el proceso de vaporización fue altamente favorecido así como la penetración del chorro. Para ambos combustibles, a medida que la presión de inyección se incrementó el SMD disminuyó y la tasa de evaporación aumentó.

----- *Palabras clave:* Chorros de combustible, atomización, vaporización, simulación.

Introduction

Due to its high efficiency, diesel engines have been the favorite power train for heavy-duty vehicles and non-road applications, and their use in light duty vehicles has been increasing.

During the last decades, the development of high-pressure direct injection combined with modern turbo-charging techniques has revolutionized the diesel engine technology. In direct injection diesel engines the fuel spray evolution significantly affects the ignition behavior, fuel consumption and exhaust emissions.

Fuel sprays are the result of high pressure-driven liquid fuel jets injected through a nozzle orifice into a combustion chamber. The jet atomizes, and then the fuel droplets evaporate and mix with air to form a reactive flow which, as a consequence of increased gas pressure and temperature, ignites and thus initiates the combustion process [1, 2].

Currently, diesel engine designers are challenged by the need to fulfill with ever more stringent emissions standards while at the same time improving engine efficiency. The achievement of these goals requires a thorough characterization of diesel sprays.

In order to study practical diesel sprays it is necessary to take into account several sub-processes such as jet atomization, drop breakup and drag, drop collision and coalescence, drop vapo-

rization, turbulent diffusion and modulation and spray/wall interactions [3].

Diesel sprays can be studied by carrying out controlled experiments or deriving mathematical models or sub-models that isolate the relevant sub-processes. Several numerical models have been developed using combinations of sub-models to describe the performance of the overall system [4-9]. However the accuracy of such approaches must be assessed by comparison with detailed experiments. Once verified, models can give insights about key processes that would be difficult to obtain in any other way, since direct measurement is often not feasible.

In an order of increasing complexity, three different model categories used in combustion research are commonly distinguished: thermodynamic (zero dimensional) models, phenomenological (quasi-dimensional) models, and multidimensional models which are utilized in so-called CFD (computational fluid dynamics) codes [10].

Multidimensional CFD-codes solve the full set of differential equations for species, mass, energy, and momentum conservation on a relatively fine numerical mesh and also include sub-models to account for the effects of turbulence [11]. As a result, these models are better suited to analyze, in greater detail, the various sub-processes of spray formation which proceed simultaneously

and interfere with each other [10]. However, they are also much more costly in terms of computer power than the other model categories.

The aim of this work is to study, using a CFD code, the effect of several variables, especially the type of fuel, on the main characteristics of a diesel spray. Several commercial CFD codes such as FIRE, STAR-CD, FLUENT or KIVA-3V, widely used for research on chemically reacting flows, offer sub-models for fuel sprays simulation [4, 12-14]. The tool used in this work is OpenFoam, which is an open-source code available in the web (www.openfoam.com). It is an object oriented code written in C++, which makes it reasonably straightforward to implement new models and fit them into the whole code structure.

The majority of the diesel spray sub-models incorporated into CFD codes have been developed for petroleum-based fuels. There are few published applications of these tools involving alternative fuels for diesel engines such as biodiesel or dimethyl ether [15, 16]. Comparing the spray characteristics of different fuels is useful in analyzing their potential to produce pollutant emissions such as particulate matter and nitrogen oxides.

Methodology

Spray sub-models

The *Kelvin-Helmholtz Rayleigh-Taylor* (KH-RT) model was selected to represent spray breakup. This model, alongside the *Taylor analogy breakup* (TAB) model, is one of the most used models in Lagrangian spray simulation [17-19]. This approach follows the droplets paths in space, although the continuous phase (gas) is not solved [9]. It should be noted that the KH-RT model was originally applied for hydrocarbon fuels. However, it is a physically based model, which means it can be extended to other fuels provided the physical properties are well defined [15].

Droplet evaporation is governed by conductive, convective and radiative heat transfer from the hot gas to the colder droplet and by simultaneous diffusive and convective mass transfer of fuel va-

por from the boundary layer at the drop surface into the gas environment. Due to the difficult task of solving the flow field in and around the many droplets of a complete spray, in CFD codes such as OpenFoam it is assumed that the droplets are ideally spherical and average flow conditions and transfer coefficients around the droplets are determined [10].

Especially in diesel engines with compact combustion chambers and high pressure injection systems spray wall impingement is an inherent sub-process of mixture formation. The so-called *reflect regime* of impingement was selected in this work. In this model the tangential velocity component of the outgoing droplet remains unchanged whereas the normal velocity component keeps its initial absolute value but changes its sign after impact [3].

The injection model used in the Lagrangian simulation was the so-called *constInjector*, which takes as input parameters the nozzle length/diameter ratio and the cone angle on which the drops will be distributed randomly [10]. The velocity of the droplets depends on the injection pressure and the pressure of the surrounding gas phase. The force acting on the droplet, causing changes in its velocity, is composed of body forces and the drag force caused by the relative velocity of the droplet to the surrounding gas phase.

Sub-models for droplet collision and coalescence, and for turbulent dispersion were not taken into account in this piece of research.

Selected fuels

The interest of this work is to test fuels of different chemical nature, especially, hydrocarbons, ethers and esters. Conventional diesel fuel is a very complex mixture of thousands of individual hydrocarbons, most with carbon numbers between 10 and 22. Biodiesel is a simpler mixture of alkyl esters of long-chain fatty acids. Dimethyl ether (DME, C_2H_6O) is the simplest ether.

Since the goal of the authors is to develop a tool for simulating diesel sprays that can be upgraded

by adding ignition and combustion sub-models, it is more practical to select well-characterized fuels that can be used as surrogates for diesel and biodiesel fuels. These fuels must have reproducible combustion characteristics that are similar to those of diesel and biodiesel. In that sense, n-heptane (NH, C_7H_{16}) and methyl butanoate (MB,

$C_5H_{10}O_2$) are recommended surrogate fuels [20-23].

The main properties of the fuels selected are listed in table 1. The majority of this data was taken from the tables for pure components of the *NRSDS* (*National Standard Reference Data System*).

Table 1 Fuel properties

<i>Property</i>	<i>DME</i>	<i>MB</i>	<i>NH</i>	<i>Units</i>
Molecular weight (W)	46.069	102.133	100.204	kg/kmol
Density (ρ) at 15 °C	667 (as liquid)	897 [24]	683 [24]	kg/m ³
Absolute viscosity at 20 °C (μ)	0.00015 (as liquid)	0.000579 [24]	0.000418 [24, 25]	Pa.s
Surface tension at 20°C (σ)	--	24.63 [26]	19.78 [25, 26]	dyne/cm
Critical temperature (Tc)	400.1	554.5	540.2	K
Critical pressure (Pc)	5.3702	3.4734	2.74	MPa
Critical volume (Vc)	0.17	0.34	0.428	m ³ /kmol
Critical compressibility factor (Zc)	0.274	0.256	0.261	Dimensionless
Flash point	--	285	269	K
Normal boiling point (Tb)	248.31	375.90	371.58	K

Simulation parameters

Three different injection pressures (40 MPa, 50 MPa y 60 MPa) and three ambient gas pressures (0.1 MPa, 1 MPa y 2 MPa) were considered.

After several sensibility tests of the model with respect to mesh size, a hexahedral mesh with square base of 41 x 41 x 200 cells (0.5 mm x 0.5 mm x 1 mm) was chosen. The injector exit was located at 0.5 mm below the center of the hexahedron top. All simulations were executed during 2 ms, with time intervals of 2.5 μ s, and data stora-

ge each 0.1 ms. In all simulations, injection was carried out at constant pressure during 1.25 ms.

The fuel injection rate was determined indirectly as a function of injection pressure, needle lift timing and discharge coefficient. The injector was characterized by a discharge coefficient of 0.9 and a nozzle diameter of 0.19 mm.

Model outputs

In order to characterize the fuel spray, three global parameters, spray tip penetration, drop mean

diameter and evaporation rate, were selected. An appropriate and commonly used drop mean diameter is the Sauter mean diameter (SMD). The SMD is the diameter of the droplet that has the same surface/volume ratio as that of the total spray.

Model validation

In order to validate the model, simulation results for the spray tip penetration were compared with experimental data about DME sprays presented by Suh and Lee [27], and results obtained using empirical correlations proposed by Hiroyasu *et al.* [28], and Sazhin *et al.* [29].

The correlations proposed by Hiroyasu *et al.* take into account the sensitivity of the spray tip position (S) as a function of time to ambient gas state and injection pressure. Equations 1 and 2 show that the initial spray tip penetration increases linearly with time (i.e., the spray tip velocity is constant) and, following jet breakup, then increases as $t^{0.5}$ [1].

$$t_{asoi} \leq t_b : \quad S = 0.39 \sqrt{\left(\frac{2\Delta P}{\rho_l}\right)} t_{asoi} \quad (1)$$

$$t_{asoi} \geq t_b : \quad S = 2.95 \left(\frac{\Delta P}{\rho_g}\right)^{0.25} \sqrt{D(t_{asoi})} \quad (2)$$

where:

$$t_b = \frac{28.65\rho_l D}{\sqrt{\rho_g \Delta P}} \quad (3)$$

and ΔP is the pressure drop across the nozzle (Pa), ρ_l and ρ_g are the liquid and gas densities, respectively (kg/m^3), D is the nozzle diameter (m), and t_{asoi} is the time measured after start of injection (s).

On the other hand, the correlation proposed by Sazhin *et al.* is given by the following expression:

$$S = 1.189 \left[\frac{1}{(1-\alpha)^{0.5}} \right]^{0.5} \left(\frac{C_d}{\tan\theta} \right)^{0.5} \left(\frac{\Delta P}{\rho_g} \right)^{0.25} D^{0.5} \quad (4)$$

where C_d is the discharge coefficient, α is the breakup coefficient, and θ is the half cone angle.

Results and discussion

In figures 1 to 3, some results obtained with the simulation model, indicating the dependence of the DME spray tip penetration as a function of time for different injection (P_{inj}) and ambient gas (P_{amb}) pressures, are compared with those obtained experimentally by Suh and Lee and predicted by the empirical correlations proposed by Hiroyasu *et al.*, and Sazhin *et al.* As can be seen, in all cases the model, as well as the correlations, is able to reproduce the trend shown by the experimental data. The model exhibits its best performance at higher injection and ambient gas pressures (see figure 3). At times before the end of injection (1.25 ms) the model tends to over predict the measured spray tip penetration.

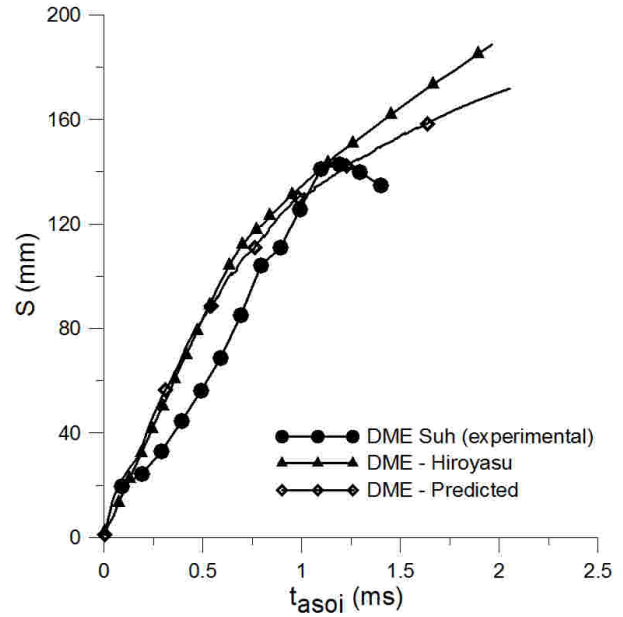


Figure 1 Spray tip penetration for DME ($P_{inj} = 40$ MPa, $P_{amb} = 0.1$ MPa)

As seen in figure 4, during earlier times before the end of injection (1.25 ms) spray tip penetration is longer for NH and slightly increases with injection pressure. This result agrees with the trend indicated by equation (1) and is a consequence of the greater pressure drop across the nozzle and the higher density of the MB as a liquid.

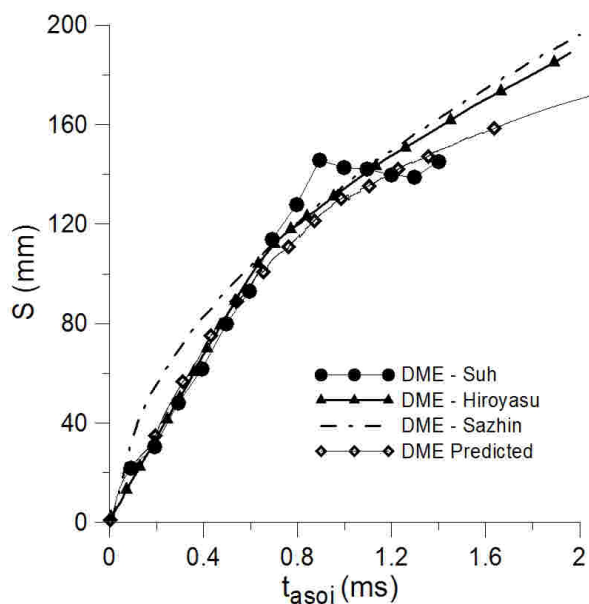


Figure 2 Spray tip penetration for DME ($P_{inj} = 60$ MPa, $P_{amb} = 0.1$ MPa)

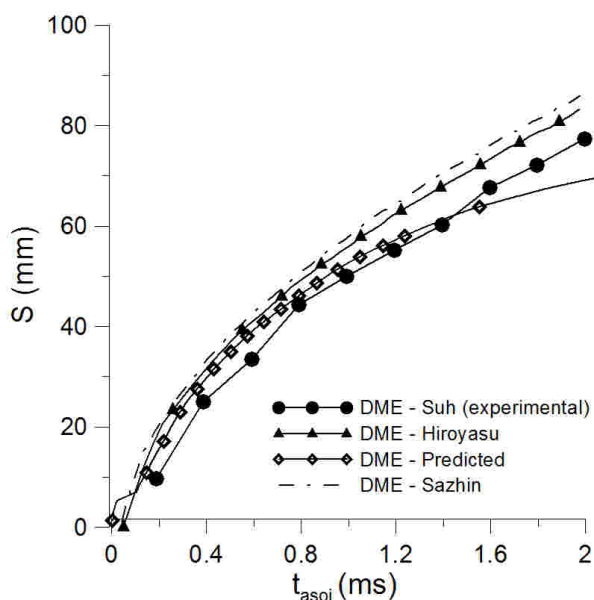


Figure 3 Spray tip penetration for DME ($P_{inj} = 60$ MPa, $P_{amb} = 2$ MPa)

On the other hand, in the later times after the end of injection, the effect of injection pressure is not significant while the trend respect to the effect of fuel type is reversed presenting a longer penetration the MB spray. Once injection stops, ambient gas density has a greater impact on spray

motion than injection pressure and liquid density (see equation 2). Additionally, it is expected that spray penetration decreases with fuel volatility.

Figures 4 to 6 show the effect of fuel type and injection pressure on spray tip penetration, Sauter mean diameter and evaporation rate.

The results obtained are in agreement with experimental data reported by several researches who argue that injection pressure has a significant effect on injection velocity (the slope of the curve $S-t$) but not on spray penetration [30].

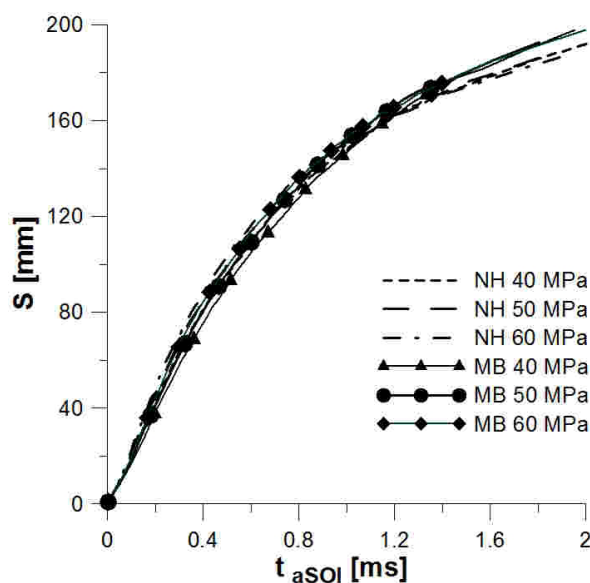


Figure 4 Spray tip penetration for NH and DME at different injection pressures ($P_{amb} = 0.1$ MPa, $T = 293$ K)

Figure 5 shows that, regarding the fuel, the Sauter mean diameter of the drops decreases with injection pressure. This result is a consequence of increasing aerodynamic interactions (increasing the relative velocity) between liquid fuel ligaments or bigger drops and the surrounding air. It can also be noted that the SMD tends to stabilize after the end of injection since there is not more generation of bigger drops at the nozzle exit. At the same injection pressure, the SMD is greater for MB since it is the fuel with higher viscosity and surface tension (see table 1). Figure 5 also shows that the effect of fuel type on the SMD is stronger than that of injection pressure.

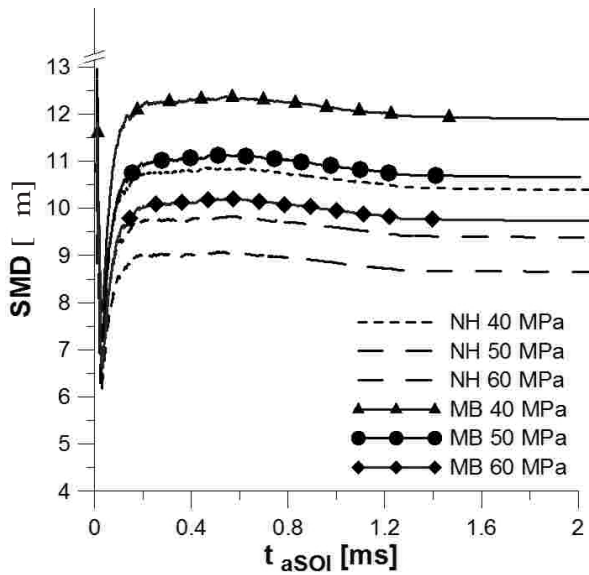


Figure 5 Sauter mean drop diameter for NH and MB at different injection pressures ($P_{amb} = 0.1 \text{ MPa}$, $T = 293 \text{ K}$)

Figure 6 shows that the evaporated mass increases with injection pressure for both fuels. As injection pressure increases the evaporation rate increases (slope of the curve) as a consequence of the smaller droplets evaporating faster (decrease in SMD). At the same injection pressure there is always more evaporated mass (more than two-fold) for NH due to its higher volatility (lower flash point and normal boiling point). As in the case of SMD, the effect of fuel type on evaporated mass is stronger than that of injection pressure.

The effect of fuel type and ambient gas pressure on spray tip penetration, SMD and evaporation rate is shown in figures 7 to 9.

As can be seen in figure 7, the effect of fuel type on spray tip penetration becomes insignificant as the ambient gas pressure increases. On the other hand, regarding the fuel type, the pressure inside the combustion chamber has a significant effect on spray tip penetration. As the ambient gas pressure increases the pressure drop across the nozzle decreases and so the spray tip penetration also decreases. In addition, an increase in the ambient gas pressure leads to an increase in the ambient

gas density and in the aerodynamic interactions and so the breakup time occurs earlier (see equation 3) decreasing the spray penetration and the SMD (figure 8). At the same ambient gas pressure the more viscous fuel generates droplets with greater SMD.

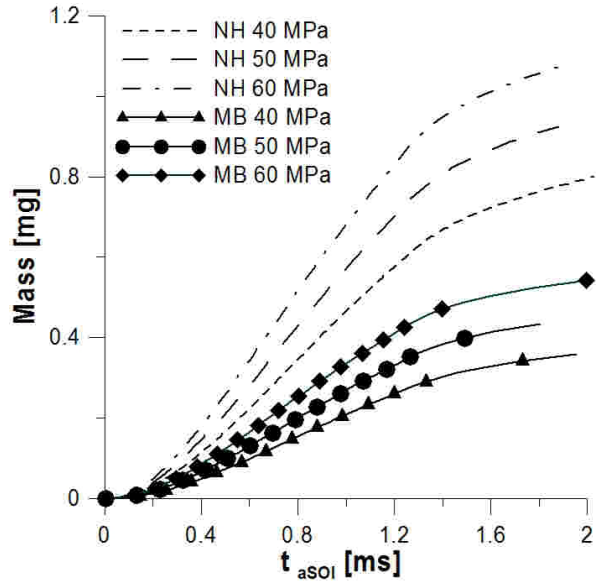


Figure 6 Evaporated mass for NH and MB at different injection pressures ($P = 0.1 \text{ MPa}$, $T = 293 \text{ K}$)

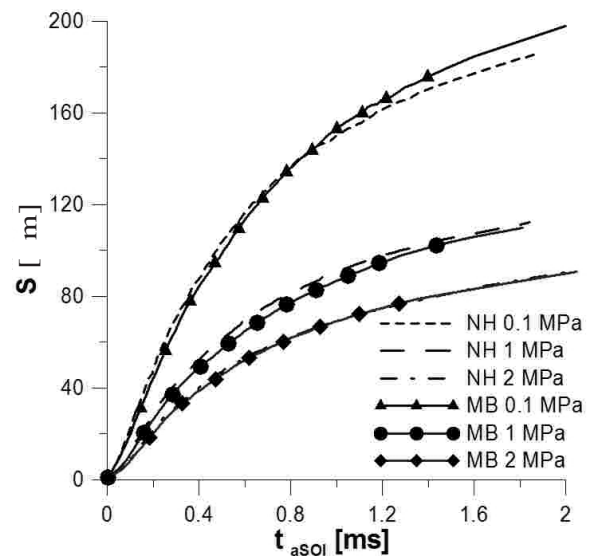


Figure 7 Spray tip penetration for NH and MB at different ambient gas pressures ($P_{inj} = 60 \text{ MPa}$, $T = 293 \text{ K}$)

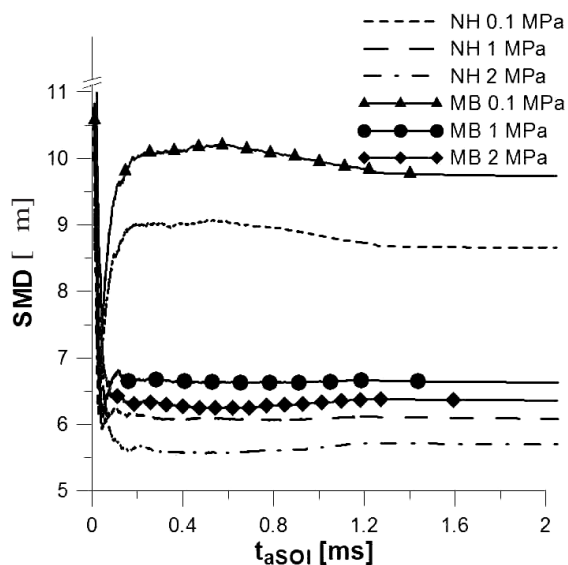


Figure 8 Sauter mean drop diameter for NH and MB at different ambient gas pressures ($P_{inj} = 60 \text{ MPa}$, $T = 293 \text{ K}$)

As seen in figure 9, as the ambient gas pressure decreases the evaporation process is highly favored. A decrease in the combustion chamber pressure leads to an increase in droplets velocity, and so the convective heat-transfer coefficient between the drop and the air increases. Figure 9 also shows the significant effect of fuel volatility on evaporation rate.

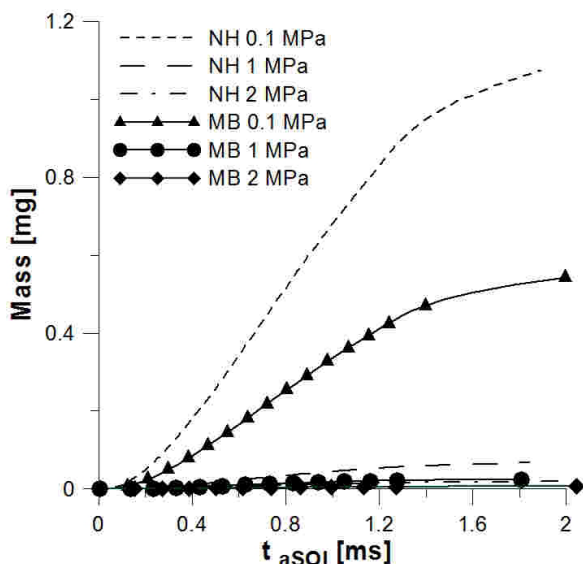


Figure 9 Evaporating rates for NH and MB at different ambient gas pressures ($P_{inj} = 60 \text{ MPa}$, $T = 293 \text{ K}$)

Conclusions

A numerical model for simulating the main sub-processes occurring in a fuel spray was developed using OpenFoam, which is an open-source CFD code. The model was able to reproduce the trend shown by experimental data of dimethyl ether spray tip penetrations reported in the literature.

The model allowed studying the effect of fuel type, injection pressure and ambient gas pressure on spray tip penetration, Sauter mean diameter (SMD) and evaporated fuel mass.

Fuel properties significantly affected the atomization and evaporation processes and in a lesser extent the spray fuel penetration. Regarding the injection and ambient gas pressures, the SMD increased with viscosity and surface tension while the evaporation rate increased with fuel volatility. At low ambient gas pressures the evaporation process was highly favored as well as the spray penetration. For both fuels, as injection pressure increased the SMD decreased and the evaporation rate increased.

References

1. J. B. Heywood, *Internal Combustion Engine Fundamentals*. Ed. McGraw-Hill. México. 1998. pp. 596-598.
2. J. R. Agudelo. *Motores diesel turboalimentados en régimen transitorio. Un análisis teórico-experimental*. Ed. Universidad de Antioquia. Medellín. 2002. pp. 77-83.
3. R. D. Reitz. "Atomization and droplet breakup, collision/coalescence and wall impingement," *Multiphase Science and Technology*. Vol. 15. 2003. pp. 343-348.
4. A. D. Gosman. "State of the art of multi-dimensional modeling of engine reacting flows," *Oil and gas science and technology – Rev. IFP*. Vol. 54. 1999. pp. 149-159.
5. J. V. Pastor, E. Encabo, S. Ruiz. "New modeling approach for fast online calculations in sprays". *SAE paper*, Vol. 2000-01-0287. 2000. pp. 1-9.
6. B. Dillies, A. Ducamin, L. Lebrere, F. Neveu. "Direct injection diesel engine simulation: a combined numerical and experimental approach from aerodynamics to combustion". *SAE paper* 1997-0880. 1997. pp. 23-48.

7. C. Chryssakis, D. N. Assanis, C. Bae. "Development and validation of a comprehensive CFD model of diesel spray atomization accounting for high Weber numbers," *SAE paper* 2006-01-1546. 2006. pp. 1-13.
8. B. Kelg. "Numerical analysis of injection characteristics using biodiesel fuel". *Fuel*. Vol. 85. 2006. pp. 2377-2387.
9. F. V. Tinaut, A. Melgar, B. Giménez. "A model of atomization of a transient evaporative spray". *SAE paper* 1999-01-0913. pp.1-10.
10. G. Stiesch. *Modeling engine spray and combustion processes*. Ed. Springer-Verlag N.Y. Inc. 2003. pp 141-149.
11. B. Reveille, A. Kleemann, S. Jay. "Towards even cleaner diesel engines: Contribution of 3D CFD tools". *Oil and gas science and technology – Rev. IFP*. Vol. 61. 2006. pp. 43-56.
12. Y. Jeong, Y. Quian, S. Campbell, K. Rhee. "Investigation of a direct injection diesel engine by high-speed spectral IR imaging and KIVA-II". *SAE paper* 941732. 1994. pp. 1-11.
13. B. Dillies, B. Cousyn, A. Ducamin. "Indirect Injection Diesel Engine Combustion Calculations: Validation and Industrial use of the KIVA-II code". *26th FISITA Congress*. Praga, 1996.
14. K. Tsao, Y. Dong, Y. Xu, "Investigation of flow field and fuel spray in a direct injection diesel engine via KIVA-II program," *SAE paper*. 961616. 1990. pp. 1-11.
15. W. Yuan, A. C. Hansen, M. E. Tat, J. H. Van Gerpen, Z. Tan. "Spray, ignition and combustion modeling of biodiesel fuels for investigating NO_x emissions". *Transactions of the ASAE*. Vol. 48. 2005. pp. 933-939.
16. K. Yamane, A. Ueta, Y. Shimamoto. "Influence of Physical and Chemical Properties of Biodiesel Fuel on Injection, Combustion and Exhaust Emission Characteristics in a DI-CI Engine". *The Fifth International Symposium on Diagnostics and Modeling of Combustion in Internal Combustion Engines (COMODIA 2001)*. Nagoya. 2001. pp. 402-409.
17. G. Pizza, Y. M. Wright, G. Weisser, K. Boulouchos. "Evaporating and non-evaporating diesel spray simulation: comparison between the ETAB and wave breakup model". *International Journal of Vehicle Design*. Vol. 45. 2007. pp. 80 - 99.
18. C. Baumgarten, G. P. Merker. "Modeling primary break-up in high-pressure diesel injection," *Motortechnische Zeitschrift (MTZ worldwide)*. Vol. 65. 2004. pp. 21-24.
19. F. X. Tanner. "Liquid jet atomization and droplet breakup modeling of non-evaporative diesel fuel sprays". *SAE paper* 1997-0050. pp. 67-80.
20. Z. Zheng, M. Yao. "Charge stratification to control HCCI: Experiments and CFD modeling with n-heptane as fuel," *Fuel*. Vol. 88. 2008. pp. 354-365.
21. E. M. Fisher, W. J. Pitz, H. J. Curran, C. K. Westbrook. "Detailed chemical kinetic mechanism for combustion of oxygenated fuels". *Proceedings of the combustion institute*. Vol. 28. 2000. pp. 1579-1586.
22. S. Gail, S. M. Sarathy, M. J. Thomson, P. Dievert, P. Dagaut. "Experimental and chemical kinetic modeling study of small methyl esters oxidation: Methyl (E)-2-butenoate and methyl butanoate". *Combustion and Flame*. Vol. 155. 2008. pp 635-650.
23. P. F. Flynn, J. E. Dec, C. K. Westbrook. "Diesel combustion: An integrated view combining laser diagnostics, chemical kinetics, and empirical validation". *SAE paper* 1999-01-0509.
24. J. S. Matos, J. L. Trenzado, E. González, R. Alcalde. "Volumetric properties and viscosities of the methyl butanoate + n-heptane + n-octane ternary system and its binary constituents in the temperature range from 283.15 to 313.15 K". *Fluid Phase Equilibria*. Vol. 186. 2001. pp 207-234.
25. B. E. Poling, J. M. Praustniz, J. P. O'Connell. *The properties of gases and liquids*. Ed. McGraw-Hill. New York. 2001. pp 278-280.
26. P. Winget, D. M. Dolney, D. J. Giesen, C. J. Cramer, D. G. Truhlar. *Minnesota Solvent Descriptor Database*. Department of Chemistry and Supercomputer Institute, University of Minnesota. Minneapolis. 1999.
27. H. K. Suh, C. S. Lee. "Experimental and analytical study on the spray characteristics of dimethyl ether (DME) and diesel fuels within a common-rail injection system in a diesel engine". *Fuel*. 2007. pp. 1-8.
28. H. Hiroyasu, M. Arai. "Fuel spray penetration and spray angle in diesel spray". *Transactions Journal SAE*. Vol. 21. 1980. pp. 5-11.
29. S. S. Sazhin, G. Geng, M. R. Heikal, "A model for fuel spray penetration". *Fuel*. Vol. 80. 2001. pp. 2171-2180.
30. D. L. Siebers. "Scaling liquid-phase fuel penetration in diesel sprays based on mixing-limited vaporization." *SAE paper* 1999-01-0528. pp. 1-24.